Metabolic intervention that reduces glucose-insulin signaling suppresses the onset and progression of neuroendocrine tumors

Yu Chen[1], Yura Takahashi[1], Tomoka Moro[1], Tomoko Tajima[1], Yukiko Sakaguchi[1], Tatsuki Yamamoto[1], Akihiko Yokoyama[2], Susumu Hijioka[3], Akane Sada[1], Yuko Tabata[1] and Rieko Ohki[1,*]

[1] Laboratory of Fundamental Oncology, National Cancer Center Research Institute, Tsukiji 5-1-1, Chuo-ku, Tokyo 104-0045, Japan.

[2] Tsuruoka Metabolomics Laboratory, National Cancer Center, Yamagata, 997-0052, Japan.

[3] Department of Hepatobiliary and Pancreatic Oncology, National Cancer Center Hospital, Tokyo 104-0045, Japan.

Running title: Repression of insulin signaling by dietary intervention suppresses neuroendocrine tumors

Key words: neuroendocrine tumor, non-functional pancreatic neuroendocrine tumor, MEN1, ketogenic diet, pituitary neuroendocrine tumor

*Correspondence:

Rieko Ohki; Tel: 81-3-3542-2511 ext. 3833, E-mail: rohki@ncc.go.jp

ABSTRACT

Insulin signaling often plays a role in the regulation of cancer including tumor initiation, progression, and response to treatment. In addition, the insulin-regulated PI3K-Akt-mTOR pathway plays an important role in the regulation of islet cell proliferation and this pathway is hyperactivated in human non-functional pancreatic neuroendocrine tumors (PanNETs). We therefore investigated the effect of a very low carbohydrate diet (ketogenic diet) on a mouse model that develops non-functional PanNETs to ask how reduced PI3K-Akt-mTOR signaling might affect the development and progression of non-functional PanNET. We found that this dietary intervention resulted in lower PI3K-Akt-mTOR signaling in islet cells and a significant reduction in PanNET formation and progression. We also found that this treatment had a significant effect on the suppression of pituitary NET development. Furthermore, we found that non-functional PanNET patients with lower blood glucose levels tend to have a better prognosis than patients with higher blood glucose levels. This preclinical study shows that a dietary intervention that results in lower serum insulin levels leads to lower insulin signal within the neuroendocrine cells and has a striking suppressive effect on the development and progression of both pancreatic and pituitary NETs.

Introduction

The pancreas serves two distinctly different functions as an exocrine organ and endocrine organ. As an endocrine organ, pancreatic islet cells release hormones and polypeptides, including insulin and glucagon, that regulate blood sugar levels and multiple other functions. When these pancreatic islet cells become cancerous, they are termed pancreatic neuroendocrine tumors (PanNETs). PanNETs are relatively rare tumors, comprising 1-2% of all pancreatic neoplasms and with an incidence of 0.43 per 100,000; however, this rate has more than doubled in the last 20-30 years [1]. The majority of PanNETs arise sporadically, but approximately 10% are associated with an underlying genetic syndrome [2]. PanNETs are divided into functional versus non-functional tumors with about 90% being classified as non-functional. Lesions should be surgically resected when possible, as this is the only potentially curative therapy. Liver metastasis is the most significant prognosis factor in the PanNET progression setting. Most patients, however, that have the metastatic disease are not candidates for resection. The majority of the drugs approved for the management of PanNET show little objective response, providing little progression-free survival or ability to shrink tumors, and thus PanNETs represent a serious unmet medical need in the clinic [3 4].

Some PanNETs arise due to a genetic disease called Multiple endocrine neoplasia type 1 (MEN1), an autosomal dominantly inherited tumor syndrome caused by germline mutations of the tumor suppressor gene *MEN1* [5]. PanNETs are the most prevalent NETs found in MEN1 patients, who will also develop NETs in other organs such as the pituitary; however, the development of a PanNET is a poor prognostic factor. Roughly 50% of patients are diagnosed with PanNETs under age 50, and since most patients have multiple non-functional PanNETs, surgery is not a therapeutic option [3]. The association between the loss of the *MEN1* gene function and the development of NETs has been confirmed by analyzing *MEN1*-deficient mice [6]. The *Men1*$^{f/f}$-RipCre^{+} mouse in which *MEN1* is ablated in pancreatic β-cells and pituitary cells is the most well-characterized MEN1 mouse model [7, 8]. These mice develop PanNETs and pituitary NETs and their use has contributed to a better understanding of these diseases in vivo.

Insulin signaling plays a role in cancer including tumor initiation, progression and response to treatment [9]. Studies of some common cancers, such as breast and pancreatic cancers, have shown that hyperinsulinemia enhances tumor development in both humans and mice, while reduced insulin levels reduces tumor development [10 11 12 13]. Several preclinical studies in mice have shown that dietary interventions leading to low insulin levels in the blood can enhance anticancer therapy and improve the outcomes of several cancers [14 15]. It is of note that a diet that reduces the serum insulin levels, i.e., a low-carbohydrate ketogenic diet, is safe and has no adverse effects in mice [16].

Pancreatic islets are exposed to high levels of insulin, which is released from β cells within the islets [17]. In addition, it has been shown that the insulin-regulated PI3K-Akt-mTOR pathway plays an important role in the regulation of islet cell proliferation and this pathway is hyperactivated in human PanNETs [18] [19] [20]. We have previously shown that hyperactivation of the PI3K-Akt-mTOR pathway caused by suppression of the tumor suppressor gene *PHLDA3*, which encodes a repressor of Akt, contributes to the formation of hyperplastic islets in mouse models and to the progression of human PanNETs [19] [20] [21] [22] [23]. These observations led us to investigate the effects of an insulin-lowering diet on PanNET initiation and progression using a newly established non-functional PanNET mouse model, which we fed with a very low carbohydrate diet (ketogenic diet). When fed a normal diet, these mice develop non-functional PanNET by the age of 45 weeks, however when fed a very low carbohydrate diet both initiation and progression of non-functional PanNET were significantly suppressed. We also found that pituitary NET development in these mice is attenuated by a ketogenic diet. We further showed that PanNET patients with higher blood glucose levels tend to have a poorer prognosis than those with lower blood glucose levels. Collectively, these results suggest a novel therapeutic and preventive approach of using a ketogenic diet to treat NET patients, including sporadic and familial non-functional PanNET and pituitary NET patients. This treatment has shown no adverse effects and provides a novel method to fulfill the unmet medical needs of non-functional PanNET and pituitary NET patients.

Results

β cell-specific *MEN1* knock-out mice that lack the exons 3-6 develop non-functional PanNETs

There are several independent β cell-specific *MEN1* knock-out mice that are similar but slightly different from one another [6]. For example, β cell-specific *MEN1*-deficient mice that lack exons 3-8 develop PanNET by 15 months of age, while mice that lack exon 3 develop PanNET by 6 months [7,8]. We made a β cell-specific *MEN1* conditional knock-out mouse line by crossing *MEN1* exons 3-6 floxed mice with RIP-Cre mice (*Men1*$^{f/f}$-RipCre^{+}) [24]. Similar to previous reports, nearly all of these mice developed PanNET by 10 months of age (Fig. 1A). As shown in Figs. 1B-1D, we found that the body weights, blood glucose levels and serum insulin levels in these mice are similar to those of wild-type mice at the same age. However, insulin expression is reduced in the islets of the *Men1*$^{f/f}$-RipCre^{+} mice at 10 months compared to the wild-type mice at the same age (Fig. 1E). It was previously reported that β cell-specific, *MEN1*-deficient mice that lack exons 3-8 or exon 3 develop functional insulinomas with significantly elevated levels of serum insulin levels [7,8]. However, we found that β cell-specific, *MEN1*-deficient mice that lack exons 3-6 develop non-functional PanNETs that resemble those found in human MEN1 patients.

A ketogenic diet suppresses PanNET development

We found that male mice lacking *MEN1* exons 3-6 in β cells develop PanNET by the age of 45 weeks. These mice have almost no abnormalities at 10 weeks (Figs. 2A-2C). In order to analyze the effect of a ketogenic diet on non-functional PanNET development, we started feeding the *Men1*$^{f/f}$-RipCre^{+} male mice with a ketogenic diet from the age of 7-13 weeks. The mice were sacrificed at age 45 weeks and the sizes of the islets were analyzed. As shown in Figs. 2A-2C, the ketogenic diet significantly suppressed the development of islet hyperplasia and PanNET. There was no significant difference in the sizes of the islets of the ketogenic diet-fed mice and wild-type mice at the same age (Fig. 2C). In addition, the sizes of the islets of *Men1*$^{f/f}$-RipCre^{+} mice fed the ketogenic diet were not significantly different from those of 10-week-old mice, showing that the ketogenic diet suppressed the enlargement of the islets during the first 35 weeks (Fig. 2C).

We next analyzed the features of the islets of the ketogenic diet-fed *Men1*$^{f/f}$-RipCre^{+} mice. As shown in Fig. 2D, islets from *Men1*$^{f/f}$-RipCre^{+} mice fed either a normal or ketogenic diet were both positive for the neuroendocrine marker chromogranin A and had lost the expression of Menin as expected. As shown in Fig. 1E, *MEN1*-deficient islets at 45 weeks of age had decreased insulin expression. However, this decrease in islet insulin expression was rescued in mice fed a ketogenic diet (Figs. 2E and 2F). Collectively these results show that the ketogenic diet dramatically suppresses the onset of non-functional PanNET.

A ketogenic diet suppresses pancreatic islet cell proliferation.

The results indicate that the lower blood glucose levels resulting from a ketogenic diet also resulted in lower insulin levels in the blood and decreased insulin signaling in islet cells. We first analyzed the body weights and blood glucose levels in 45-week-old mice fed a normal versus ketogenic diet ad libitum. As shown in Figs. 3A and 3B, blood glucose levels were significantly lower in the mice fed a ketogenic diet, while there were no significant differences in body weights. We next performed a food tolerance test using fasted mice and analyzed blood glucose and serum insulin levels 1.5 hrs post food intake. While there was a significant increase in blood glucose and high insulin secretion in the mice refed a normal diet, these increases in blood glucose and insulin were not detected in mice fed a ketogenic diet (Figs. 3C and 3D). It was also shown that insulin signaling (P-S6 and P-mTOR) is attenuated in the islet cells of mice fed a ketogenic diet (Figs. 3E-3H). Since insulin signaling is closely related to islet cell proliferation, it is expected that decreased insulin levels in the blood should result in decreased islet cell proliferation. As shown in Figs. 3I-3K, the number of Ki67-positive proliferating cells is lower and the expression of p27, a representative cell cycle inhibitor, was higher in the islets of mice fed a ketogenic diet. These data show that the ketogenic diet suppressed the proliferation of *MEN1*-deficient islet cells.

A ketogenic diet suppresses PanNET progression.

As the ketogenic diet was found to suppress the onset and development of PanNETs in *Men1*$^{f/f}$-RipCre^{+} mice, we next analyzed whether this diet also suppresses the progression of PanNETs. At 30 weeks of age, *MEN1*-deficient islets were found to be significantly larger than wild-type islets (Fig. 4A): the average size of the largest 10 islets of *Men1*$^{f/f}$-RipCre^{+} mice at 30 weeks of age was 0.17 mm^2, while those from wild type mice averaged 0.028 mm^2. We therefore started feeding the 30-week-old *Men1*$^{f/f}$-RipCre^{+} mice a ketogenic diet. When the islet sizes were subsequently analyzed at age 45 weeks, the islet sizes of the mice fed a ketogenic from 30 weeks were significantly smaller than those of mice fed a normal diet (Figs. 4B-4D). Furthermore, the islet sizes were not significantly different from those of 30-week-old *Men1*$^{f/f}$-RipCre^{+} mice, showing that the ketogenic diet suppressed the progression of PanNET for 15 weeks when the mice were fed this diet.

A ketogenic diet suppresses pituitary NET development.

Men1$^{f/f}$-RipCre^{+} mice develop not only PanNETs but also pituitary NETs. Pituitary NET development is more enhanced in female mice and most of the female mice develop pituitary NETs by the age of 45 weeks. We therefore analyzed the effect of a ketogenic diet on pituitary NET development in 45-week-old female *Men1*$^{f/f}$-RipCre^{+} mice. We started feeding the *Men1*$^{f/f}$-RipCre^{+} female mice with a ketogenic diet from the age of 10-13 weeks. As shown in Figs. 5A-5C, a ketogenic diet significantly suppressed pituitary NET development in these mice. It has been

168 reported that *MEN1*-deficient mice frequently develop prolactin-positive pituitary NETs. This
169 previous report was confirmed, and most of the *MEN1*-deficient mice fed a normal diet developed
170 prolactin-positive tumors (Figs. 5D and 5E). Within the pituitary NET of the mouse fed a normal
171 diet, accumulation of prolactin-positive cells was observed, while no cells were positive for TSH,
172 another pituitary hormone. On the other hand, the distribution of prolactin- and TSH-producing cells
173 were similar to those of wild type mice, and the clonal expansion of prolactin- and TSH-producing
174 cells was not evident in the pituitaries of mice fed a ketogenic diet from 10 weeks of age (Figs. 5D
175 and 5E).
176 As shown in Fig. S1, the median survival of female *Men1*$^{f/f}$-RipCre^{+} mice is 56 weeks, and these mice
177 die from pituitary NETs. We, therefore, fed the mice a ketogenic diet to the age of 55 weeks and
178 analyzed the size of the pituitaries. As shown in Figs. 5F and 5G, ketogenic diet significantly
179 suppressed the pituitary NET development until the age of 55 weeks. The sizes of the pituitaries of
180 55-week-old mice were similar to those of the 45-week-old mice. Collectively, these results show
181 that a ketogenic diet also suppressed pituitary NET development and contribute to the extension of the
182 life of these mice.
183
184 **The relationship between PanNET patient prognosis and blood glucose level**
185 We next analyzed the relationship between overall survival and blood glucose levels in 56 patients
186 who had been pathologically diagnosed as having non-functional PanNETs (Grade 1-3) and those who
187 had undergone chemotherapy. Patients who developed multiple primary tumors were excluded from
188 the analysis. The American Diabetes Association has determined that a fasting blood glucose level
189 from 100 to 125 mg/dl is an indication of a prediabetic state [25]. Therefore, high blood glucose levels
190 were defined in our study as blood glucose levels higher than 100 mg/dl. The median blood glucose
191 levels in the low and high blood glucose groups were 92 mg/dl (76–100 mg/dl) and 121 mg/dl (101–
192 245 mg/dl), respectively, and in the high blood glucose level group, 16 (40%) of 40 patients had blood
193 glucose level greater than 125 mg/dl. As shown in Fig. 6A, there was a tendency for patients with
194 lower blood glucose levels to have a better prognosis (p=0.16). On the other hand, when major
195 clinicopathological characteristics are classified into low and high blood glucose level groups, as listed
196 in Fig. 6B, the distributions of age, sex and tumor grade were not significantly different between the
197 two groups. For patients who had undergone chemotherapy, there was no significant bias between
198 the blood glucose high and low groups for the various chemotherapeutic regimens, also listed in Fig.
199 6C. Collectively, these data suggest that high blood glucose induces the progression of PanNETs.
200

Discussion

In this study, we have shown that the metabolic intervention of a very low carbohydrate diet (ketogenic diet) could significantly suppress both the initiation and progression of non-functional PanNET and pituitary NET in a mouse model. Recent advances in the understanding of the molecular factors involved in pancreatic and pituitary NETs have led to new antitumor treatments, including reagents acting on specific molecular targets. For example, inhibitors of receptor tyrosine kinases and mTOR are in clinical use for the treatment of PanNETs, however they may have limited efficacy and patients often stop responding to these inhibitors [26]. The most frequently used PanNET mouse model used for preclinical testing of therapies is a RipTag2 mouse model, which expresses the SV40 T antigen under the control of insulin promoter and develops functional PanNETs [27]. With this functional PanNET mouse model, it has been shown that several molecular targeted drugs such as an anti-VEGF monoclonal antibody (targeting the angiogenic pathways) or nintedanib (targeting VEGF, PDGF, and fibroblast growth factor) have anti-tumorigenic effects [28] [29] [30]. However, there have been no preclinical studies involving mouse models of non-functional PanNETs. We have established a non-functional PanNET mouse model and shown that by maintaining low insulin signaling, it is possible to prevent and suppress the progression of non-functional PanNETs. We have shown that this dietary intervention is also effective for pituitary NETs. It has been reported that a low-carbohydrate ketogenic diet is safe and has no adverse effects in mice and can improve the effectiveness of some anticancer therapies [14] [15] [16]. Therefore, it would be of great interest in future studies to test combinations of a ketogenic diet with other anticancer therapies used for PanNETs and pituitary NETs.

The results shown in this study can be translated not only to sporadic but also to familial non-functional PanNETs and pituitary NETs. In MEN1 patients that develop familial NETs, non-functional PanNETs are highly prevalent and are the major cause of premature MEN1-related death[26]. Surgery has been the only curative option for nonfunctioning PanNETs, however, since MEN1 patients often have multiple PanNETs that occur at a younger age and have a higher metastatic potential, surgery is not always possible. Although clinical guidelines recommend early detection by genetic testing of asymptomatic relatives of MEN1-mutated patients within the first decade of life, there is currently no effective method of prevention for these patients. However, this preclinical study shows that dietary intervention with a very low carbohydrate diet is effective in preventing nonfunctioning PanNET in mice, and this method may be applicable to MEN1 patients.

This dietary intervention is effective not only for the prevention of PanNETs but also for the suppression of PanNET progression, and has no adverse side effects. We also showed that higher blood glucose levels are related to poorer prognosis of PanNET patients that are receiving

237 chemotherapy. It has also been reported that high pre-operative blood glucose predicts a poor
238 prognosis in PanNET patients [31]. In addition, metformin, a drug that reduces blood glucose levels,
239 enhances the effect of chemotherapy in PanNET patients [32]. These results suggests that by lowering
240 blood glucose, PanNET progression can also be suppressed in humans. Future clinical studies to
241 investigate the effectiveness of this method for both familial and sporadic human non-functional
242 PanNETs and pituitary NETs should be of great interest. It is also possible that this treatment could
243 be applied to other types of cancers including various familial cancers that are dependent on the
244 insulin-regulated PI3K-Akt-mTOR pathway, and could represent the first effective prevention method
245 that does not have adverse effects.
246

247 **Materials and Methods**

248

249 **Mice used in this study**

250 Mouse experiments were performed in a specific pathogen-free environment at the National Cancer
251 Center animal facility according to institutional guidelines and all the animal experiments were
252 approved by the Committee for Ethics in Animal Experimentation at the National Cancer Center (T17-
253 002-C01 and T17-011-M03). Pancreatic β-cell-specific *Men1* deficient mice were generated by
254 crossing mice carrying the floxed allele (*Men* $^{f/f}$) with RIP-Cre transgenic mice expressing the Cre
255 recombinase under the control of the rat insulin II promoter (B6.Cg-Tg(Ins2-cre)25Mgn/J), termed
256 *Men1*$^{f/f}$-RipCre^{+} mice [24 33].

257

258 **Blood glucose and Plasma Insulin Measurement.**

259 Blood glucose levels were determined with blood samples from tail vein punctures in mice using a
260 Glucose pilot instrument (Aventir Biotech, Carlsbad, CA), according to the manufacturer's protocol.
261 Plasma insulin levels were determined with blood samples from the inferior vena cava in mice using
262 the Morinaga Ultra Sensitive Mouse Insulin Elisa Kit (Morinaga Institute of Biological Science, Inc.,
263 Tokyo, Japan), according to the manufacturer's protocol .

264

265 **Immunohistochemistry (IHC)**

266 IHC was performed basically as described according to the manufacturer's instructions [19]. In brief,
267 after deparaffinization, tissues sections underwent antigen retrieval by autoclaving slides in 10 mM
268 citrate buffer (pH 6.0). Sections were pretreated with 3 % H_2O_2 for inactivation of endogenous
269 peroxidase. The primary antibodies used in the study were; rabbit anti-Ki67 monoclonal antibody
270 (SP6, Novus Biologicals) diluted 1:200, rabbit anti-Chromogranin A polyclonal antibody (Thermo
271 Scientific) diluted 1:200, rabbit anti-P-S6 (#5364, CST) diluted 1:500, rabbit anti-P-mTOR (#2976,
272 CST) diluted 1:100, rabbit anti-p27 (C19, Santacruz) diluted 1:1000, rabbit anti-rat Prolactin (the
273 Institute for Molecular and Cellular Regulation, Gunma University) diluted 1:5000, rabbit anti-rat
274 TSH (the Institute for Molecular and Cellular Regulation, Gunma University) diluted 1:5000. As
275 secondary antibodies, iotinylated anti-rabbit IgG antibody (VECTOR Laboratories) were used. We
276 also used SignalStain Boost Detection Reagent (HRP, Rabbit #8114) for CST antibodies. We used
277 3,3'-diaminobenzidine tetrahydrochloride (DAB; Muto Pure Chemicals) as the substrate chromogen.
278 The sections were counter-stained with hematoxylin. For fluorescent immunohistochemical staining
279 of insulin, glucagon and Menin, nonspecific interactions were blocked for 1h using a goat serum
280 solution. The primary antibodies were: guinea pig anti-insulin polyclonal antibody (Abcam) diluted
281 1:400, mouse anti-glucagon monoclonal antibody (SIGMA-ALDRICH) diluted 1:750, rabbit anti-
282 Menin polyclonal antibody (Bethyl Laboratories, A300-105A) diluted 1:3000 with Signal Enhancer

283 HIKARI (NACALAI TESQUE). These were applied to the slides and incubated overnight at 4 °C.
284 As secondary antibodies, Alexa Fluor 546 goat anti-rabbit IgG antibody (Invitrogen) diluted 1:500 and
285 Alexa Fluor 546 or 594 goat anti-guinea pig IgG antibody (Invitrogen) diluted 1:1000 with PBST-
286 BSA were applied to the slides and incubated 3 hrs at RT. For mouse antibodies, the Vector MOM
287 immunodetection kit was used based on the protocol specified by the manufacturer (Vector
288 Laboratories). Images were taken and analyzed with an HS All-in-one Fluorescence microscope BZ-
289 9000 (KEYENCE). Image analyses were also performed using ImageJ software (imageJ.net).
290 Additionally, we used the color thresholding image adjustment employing the Colour Deconvolution
291 plugin (imagej.net/Colour_Deconvolution). We used an optimized immunohistochemistry image
292 processing protocol for DAB staining to semi-quantitatively analyze protein expression, as previously
293 described [34].
294
295 **Quantitative measurement of islet and pituitary morphology.**
296 Islet area, islet nuclei number and pituitary area were measured from hematoxylin and eosin-stained
297 pancreas sections, and Ki67-positive cells were counted from immunohistochemically stained
298 pancreas sections using TissueFAXS (TissueGnostics) and an HS All-in-one Fluorescence microscope
299 BZ-9000 (Keyence).
300
301 **Patients analyzed in the study.**
302 A retrospective cohort study was conducted consisting of 56 patients who had been pathologically
303 diagnosed with PanNETs and those that had undergone chemotherapy between July 2014 to August
304 2021 at National Cancer Center Hospital. Chemotherapies included: octreotide, lanreotide,
305 everolimus, sunitinib, streptozotocin, lanreotide+everolimus, lanreotide+sunitinib and others
306 (CDDP+CPT-11, GEM+nabPTX or PRRT). Inclusion criteria were as follows: (i) patients diagnosed
307 with PanNET; (ii) patients with follow-up data; (iii) patients with blood glucose data before the
308 treatments. Cases excluded were (i) patients diagnosed with functional PanNETs or (ii) patients that
309 had developed multiple primary tumors. This study was approved by the Institutional Review Board
310 of the National Cancer Center, Tokyo (approval number; 2013-023). Clinical and pathological data
311 were obtained through a detailed retrospective review of the medical records of all patients with
312 PanNET. According to the Standards of Medical Care in Diabetes 2022 issued by the American
313 Diabetes Association [25], a fasting blood glucose (FBG) level from 100 to 125 mg/dl is an indication of
314 a prediabetic state. Therefore, high blood glucose levels are defined as blood glucose levels higher
315 than 100 mg/dl. Overall survival (OS) was defined as the length of time (in days) from the beginning
316 of treatment to death from any cause.
317
318 **Statistical analysis.**

319 Data were calculated and shown as mean ±SEM. Comparisons between the samples were performed
320 by Student *t* test or by one-way ANOVA multiple comparisons using Prism software (version 6).
321 Survival data were analyzed using Prism software (version 6), and Kaplan–Meyer plots were drawn.
322 Statistical significance was defined as $p<0.05$.
323

CONFLICT OF INTEREST

The authors state no conflict of interest.

ACKNOWLEDGMENTS

We thank Dr. Marc Lamphier for critical reading of the manuscript. Y.C. is a JSPS International Research fellow. This work was carried out by the joint research program of the Institute for Molecular and Cellular Regulation, Gunma University. This study was partly supported by a Grant-in-Aid for Scientific Research (B, #20H03523 to R.O.), Grant-in-Aid for Scientific Research (C, #22K07181 to Yuko T.) and Grant-in-Aid for Young Scientist (B) (#19K16732 to Y.C.) from MEXT of Japan; P-Direct and P-Create from AMED of Japan (R.O.); Grant-in-Aid for JSPS fellow (# 20F20414 to R.O. and Y.C.); research grants of the Okinaka Memorial Institute for Medical Research (R.O.), the Life Science Foundation of Japan (R.O.), Pancreas Research Foundation of Japan (Y.C.) and Ichiro Kanehara Foundation for the promotion of Medical Sciences and Medical Care (Y.C.).

AUTHOR CONTRIBUTIONS

Conceptualization: RO; Formal Analysis: YC, YuraT, TM, TT, YS, TY, SH, AS, YukoT, RO; Investigation and Methodology: YC, YuraT, TM, TT, YS, TY, AY, SH, AS, YukoT, RO; Funding acquisition: YC, YukoT, RO; Supervision: RO; Writing – original draft; RO, review & editing: YC, YuraT, TM, TT, YS, TY, AY, SH, AS, YukoT, RO.

344 **References**

345 1. McKenna LR, Edil BH. Update on pancreatic neuroendocrine tumors. *Gland Surg* **3**, 258-275
346 (2014).
347

348 2. de Wilde RF, Edil BH, Hruban RH, Maitra A. Well-differentiated pancreatic neuroendocrine
349 tumors: from genetics to therapy. *Nat Rev Gastroenterol Hepatol* **9**, 199-208 (2012).
350

351 3. Mpilla GB, Philip PA, El-Rayes B, Azmi AS. Pancreatic neuroendocrine tumors: Therapeutic
352 challenges and research limitations. *World J Gastroenterol* **26**, 4036-4054 (2020).
353

354 4. Jensen RT*, et al.* Unmet Needs in Functional and Nonfunctional Pancreatic Neuroendocrine
355 Neoplasms. *Neuroendocrinology* **108**, 26-36 (2019).
356

357 5. van Treijen MJC, van Beek DJ, van Leeuwaarde RS, Vriens MR, Valk GD. Diagnosing
358 Nonfunctional Pancreatic NETs in MEN1: The Evidence Base. *J Endocr Soc* **2**, 1067-1088 (2018).
359

360 6. Wiedemann T, Pellegata NS. Animal models of multiple endocrine neoplasia. *Mol Cell Endocrinol*
361 **421**, 49-59 (2016).
362

363 7. Crabtree JS*, et al.* Of mice and MEN1: Insulinomas in a conditional mouse knockout. *Mol Cell*
364 *Biol* **23**, 6075-6085 (2003).
365

366 8. Bertolino P, Tong WM, Herrera PL, Casse H, Zhang CX, Wang ZQ. Pancreatic beta-cell-specific
367 ablation of the multiple endocrine neoplasia type 1 (MEN1) gene causes full penetrance of
368 insulinoma development in mice. *Cancer Res* **63**, 4836-4841 (2003).
369

370 9. Hopkins BD, Goncalves MD, Cantley LC. Insulin-PI3K signalling: an evolutionarily insulated
371 metabolic driver of cancer. *Nat Rev Endocrinol* **16**, 276-283 (2020).
372

373 10. Novosyadlyy R*, et al.* Insulin-mediated acceleration of breast cancer development and progression
374 in a nonobese model of type 2 diabetes. *Cancer Res* **70**, 741-751 (2010).
375

376 11. Gallagher EJ, LeRoith D. Hyperinsulinaemia in cancer. *Nat Rev Cancer* **20**, 629-644 (2020).
377

378 12. Nencioni A, Caffa I, Cortellino S, Longo VD. Fasting and cancer: molecular mechanisms and
379 clinical application. *Nat Rev Cancer* **18**, 707-719 (2018).

380
381 13. Zhang AMY, *et al.* Endogenous Hyperinsulinemia Contributes to Pancreatic Cancer Development.
382 *Cell Metab* **30**, 403-404 (2019).
383
384 14. Hopkins BD, *et al.* Suppression of insulin feedback enhances the efficacy of PI3K inhibitors.
385 *Nature* **560**, 499-503 (2018).
386
387 15. Taylor SR, Falcone JN, Cantley LC, Goncalves MD. Developing dietary interventions as therapy
388 for cancer. *Nat Rev Cancer*, (2022).
389
390 16. Douris N, *et al.* Adaptive changes in amino acid metabolism permit normal longevity in mice
391 consuming a low-carbohydrate ketogenic diet. *Biochim Biophys Acta* **1852**, 2056-2065 (2015).
392
393 17. Johnson JD, Alejandro EU. Control of pancreatic beta-cell fate by insulin signaling: The sweet
394 spot hypothesis. *Cell Cycle* **7**, 1343-1347 (2008).
395
396 18. Elghazi L, Balcazar N, Bernal-Mizrachi E. Emerging role of protein kinase B/Akt signaling in
397 pancreatic beta-cell mass and function. *Int J Biochem Cell Biol* **38**, 157-163 (2006).
398
399 19. Ohki R, *et al.* PHLDA3 is a novel tumor suppressor of pancreatic neuroendocrine tumors. *Proc*
400 *Natl Acad Sci U S A* **111**, E2404-2413 (2014).
401
402 20. Chen Y, Ohki R. p53-PHLDA3-Akt Network: The Key Regulators of Neuroendocrine
403 Tumorigenesis. *Int J Mol Sci* **21**, (2020).
404
405 21. Kawase T, *et al.* PH domain-only protein PHLDA3 is a p53-regulated repressor of Akt. *Cell* **136**,
406 535-550 (2009).
407
408 22. Sakata N, *et al.* Pleckstrin homology-like domain family A, member 3 (PHLDA3) deficiency
409 improves islets engraftment through the suppression of hypoxic damage. *PLoS One* **12**, e0187927
410 (2017).
411
412 23. Takikawa M, Ohki R. A vicious partnership between AKT and PHLDA3 to facilitate
413 neuroendocrine tumors. *Cancer Sci* **108**, 1101-1108 (2017).
414
415 24. Hughes CM, *et al.* Menin associates with a trithorax family histone methyltransferase complex

and with the hoxc8 locus. *Mol Cell* **13**, 587-597 (2004).

25. American Diabetes Association Professional Practice C. 2. Classification and Diagnosis of Diabetes: Standards of Medical Care in Diabetes-2022. *Diabetes Care* **45**, S17-S38 (2022).

26. Brandi ML, Agarwal SK, Perrier ND, Lines KE, Valk GD, Thakker RV. Multiple Endocrine Neoplasia Type 1: Latest Insights. *Endocr Rev* **42**, 133-170 (2021).

27. Hanahan D. Heritable formation of pancreatic beta-cell tumours in transgenic mice expressing recombinant insulin/simian virus 40 oncogenes. *Nature* **315**, 115-122 (1985).

28. Casanovas O, Hicklin DJ, Bergers G, Hanahan D. Drug resistance by evasion of antiangiogenic targeting of VEGF signaling in late-stage pancreatic islet tumors. *Cancer Cell* **8**, 299-309 (2005).

29. Sennino B*, et al.* Suppression of tumor invasion and metastasis by concurrent inhibition of c-Met and VEGF signaling in pancreatic neuroendocrine tumors. *Cancer Discov* **2**, 270-287 (2012).

30. Bill R*, et al.* Nintedanib Is a Highly Effective Therapeutic for Neuroendocrine Carcinoma of the Pancreas (PNET) in the Rip1Tag2 Transgenic Mouse Model. *Clin Cancer Res* **21**, 4856-4867 (2015).

31. Gong Y*, et al.* High pre-operative fasting blood glucose levels predict a poor prognosis in patients with pancreatic neuroendocrine tumour. *Endocrine* **71**, 494-501 (2021).

32. Vitali E*, et al.* Metformin and Everolimus: A Promising Combination for Neuroendocrine Tumors Treatment. *Cancers (Basel)* **12**, (2020).

33. Postic C*, et al.* Dual roles for glucokinase in glucose homeostasis as determined by liver and pancreatic beta cell-specific gene knock-outs using Cre recombinase. *J Biol Chem* **274**, 305-315 (1999).

34. Capodanno Y*, et al.* Cross-talk among MEN1, p53 and Notch regulates the proliferation of pancreatic neuroendocrine tumor cells by modulating INSM1 expression and subcellular localization. *Neoplasia* **23**, 979-992 (2021).

452 **Figure legends**

453

454 **Fig. 1 β cell-specific *MEN1* knock-out mice develop non-functional PanNETs**

455 **A.** Pancreatic sections of 45-week-old wild-type mice and *Men1*$^{f/f}$-RipCre^{+} mice fed a normal diet
456 were stained with HE.

457 **B, C.** Body weights (B) and blood glucose levels (C) of 45-week-old wild-type (N=19) or *Men1*$^{f/f}$-
458 RipCre^{+} (N=21) mice fed a normal diet. Mice were fed ad libitum.

459 **D.** Serum insulin levels of 45-week-old wild-type (N=19) or *Men1*$^{f/f}$-RipCre^{+} mice fed a normal diet
460 (N=18). Mice were fed ad libitum.

461 **E.** Pancreatic sections of 45-week-old wild-type or *Men1*$^{f/f}$-RipCre^{+} mice fed a normal diet were
462 stained with anti-insulin and anti-glucagon.

463

464 **Fig. 2 Ketogenic diet suppresses non-functional PanNET development.**

465 **A.** Pancreatic sections of 45-week-old wild-type mice fed a normal diet, *Men1*$^{f/f}$-RipCre^{+} mice fed a
466 normal diet or *Men1*$^{f/f}$-RipCre^{+} mice fed a ketogenic diet from 8 weeks of age were stained with HE.
467 HE staining of pancreatic sections of 10-week-old *Men1*$^{f/f}$-RipCre^{+} mice fed a normal diet is also
468 shown.

469 **B.** Islet areas of 45-week-old wild-type mice fed a normal diet (N=6), *Men1*$^{f/f}$-RipCre^{+} mice fed a
470 normal diet (N=14) or *Men1*$^{f/f}$-RipCre^{+} mice fed a ketogenic diet from 7-13 weeks of age (N=13), and
471 10-week-old *Men1*$^{f/f}$-RipCre^{+} mice fed a normal diet (N=4) were analyzed. The areas of the top 10
472 largest islets were calculated and the means of the 10 islet areas were obtained for each mouse.

473 **C.** Statistical analysis of the average islet sizes of each group of mice was performed. P values were
474 obtained using the one-way ANOVA test. The age of the mice sacrificed are shown in parenthesis.

475 **D.** Pancreatic sections of 45-week-old wild-type mice fed a normal diet, *Men1*$^{f/f}$-RipCre^{+} mice fed a
476 normal diet or ketogenic diet from 8 weeks of age were stained with HE, anti-Chromogranin A and
477 anti-Menin.

478 **E, F.** Pancreatic sections of 45-week-old wild-type mice fed a normal diet, *Men1*$^{f/f}$-RipCre^{+} mice fed
479 a normal diet or ketogenic diet from 8 weeks of age were stained with insulin. Relative intensities
480 of insulin staining from 3 mice of each group (total 9-12 islets) were calculated and shown in Graph
481 F.

482

483 **Fig. 3 Ketogenic diet suppresses pancreatic islet cell proliferation.**

484 **A, B.** Body weights (A) and blood glucose levels (B) of 45-week-old *Men1*$^{f/f}$-RipCre^{+} mice fed a
485 normal diet (N=18) or ketogenic diet (N=32). Mice were fed ad libitum.

486 **C, D.** Blood glucose levels (C) and serum insulin levels (D) of 20-week-old *Men1*$^{f/f}$-RipCre^{+} mice fed
487 a normal diet (N=4) or ketogenic diet from 10 weeks of age (N=3). Samples were obtained from the

488 indicated numbers (N) of fasted mice (mice fasted for overnight to 41 hrs) refed the usual meal for 1.5
489 hrs.
490 **E-G.** Mice were treated as in C and pancreatic sections of mice refed a normal diet or ketogenic diet
491 were stained with HE, anti-P-S6 (E) and anti-P-mTOR (F). Relative intensities of P-S6 staining from
492 5 (normal diet) and 4 (ketogenic diet) islets were calculated and shown in graph G. Relative
493 intensities of P-mTOR staining from 4 (normal diet) and 4 (ketogenic diet) islets were calculated and
494 shown in graph H.
495 **I-K.** Pancreatic sections of 30-week-old *Men1*$^{f/f}$-RipCre^{+} mice fed a normal diet or ketogenic diet from
496 10 weeks of age were stained with HE, anti-Ki67 and anti-p27 (I). Total and Ki67 positive nuclei
497 numbers from 4 islets were counted and shown in Graph J. Relative intensities of p27 staining from
498 3 islets were calculated and shown in Graph K.
499
500 **Fig. 4 Ketogenic diet suppresses PanNET progression.**
501 **A.** Islet areas of 30-week-old wild-type mice and *Men1*$^{f/f}$-RipCre^{+} mice fed a normal diet were
502 analyzed. The areas of the top 10 largest islets were calculated and the means of the 10 islet areas
503 were obtained for each mouse.
504 **B.** Pancreatic sections of 45-week-old *Men1*$^{f/f}$-RipCre^{+} mice fed a normal diet or ketogenic diet from
505 30 weeks of age were stained with HE. HE staining of pancreatic sections of 30-week-old *Men1*$^{f/f}$-
506 RipCre^{+} mice fed a normal diet is also shown.
507 **C.** Islet areas of 45-week-old *Men1*$^{f/f}$-RipCre^{+} mice fed a normal diet or ketogenic diet from 30 weeks
508 of age, and 10- or 30-week-old *Men1*$^{f/f}$-RipCre^{+} mice fed a normal diet were analyzed as in A.
509 **D.** Statistical analysis of the average islet sizes of each group of mice was performed. P values were
510 obtained using the one-way ANOVA test. The age of the mice sacrificed are shown in parenthesis.
511
512 **Fig. 5 Ketogenic diet suppresses pituitary NET development.**
513 **A.** Pituitary sections of 45-week-old wild-type mice fed a normal diet, *Men1*$^{f/f}$-RipCre^{+} mice fed a
514 normal diet or ketogenic diet from 10 weeks of age were stained with HE.
515 **B.** Pituitary sizes of 45-week-old wild-type mice fed a normal diet, *Men1*$^{f/f}$-RipCre^{+} mice fed a normal
516 diet or ketogenic diet from 10-13 weeks of age were analyzed. Pituitaries of 10-week-old *Men1*$^{f/f}$-
517 RipCre^{+} mice fed a normal diet were also analyzed.
518 **C.** Statistical analysis of the pituitary sizes of each group of mice was performed. P values were
519 obtained using the one-way ANOVA test. The age of the mice sacrificed are shown in parenthesis.
520 **D, E.** Pituitary sections of 45-week-old wild-type mice fed a normal diet and *Men1*$^{f/f}$-RipCre^{+} mice
521 fed a ketogenic diet from 13 weeks of age were stained with anti-prolactin (D) and anti-TSH (E)
522 antibodies.
523 **F.** Pituitary sizes of 55-week-old *Men1*$^{f/f}$-RipCre^{+} mice fed a normal diet or ketogenic diet from 10-13

524 weeks of age were analyzed and compared to those of 45-week-old mice.

525 **G.** Statistical analysis of the pituitary sizes of each group of mice was performed as in C.

526

527 **Fig. 6 The prognosis of PanNET patients having lower blood glucose levels are better than those**

528 **having higher blood glucose levels.**

529 **A.** Overall survival of patients with high and low fasting blood glucose levels (N=56).

530 **B.** Baseline characteristics of patients analyzed are shown.

531 **C.** Chemotherapeutic regimens of patients analyzed are shown.

532

533

534

535 **Supplementary Figure legends**

536

537 **Fig. S1 Kaplan–Meier plots of overall survival of the female *Men1*$^{f/f}$-RipCre^{+} mice.**

538 In total, 42 female *Men1*$^{f/f}$-RipCre^{+} mice fed a normal diet were analyzed.

Fig. 1

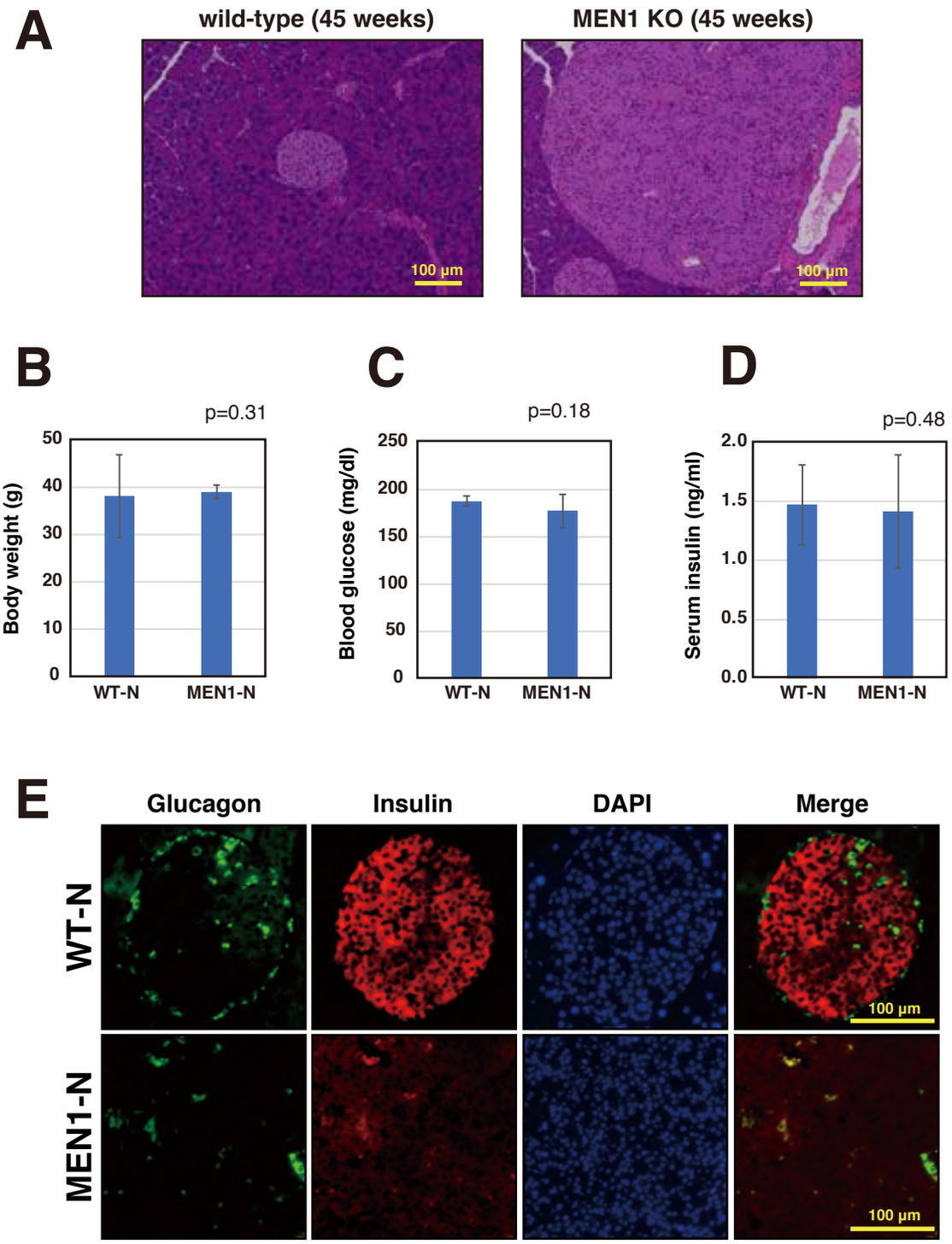
A
wild-type (45 weeks)
MEN1 KO (45 weeks)
100 μm
100 μm
B
p=0.31
Body weight (g)
50
40
30
20
10
0
WT-N
MEN1-N
C
p=0.18
Blood glucose (mg/dl)
250
200
150
100
50
0
WT-N
MEN1-N
D
p=0.48
Serum insulin (ng/ml)
2.0
1.5
1.0
0.5
0.0
WT-N
MEN1-N
E
Glucagon
Insulin
DAPI
Merge
WT-N
MEN1-N
100 μm
100 μm

Fig. 2

A

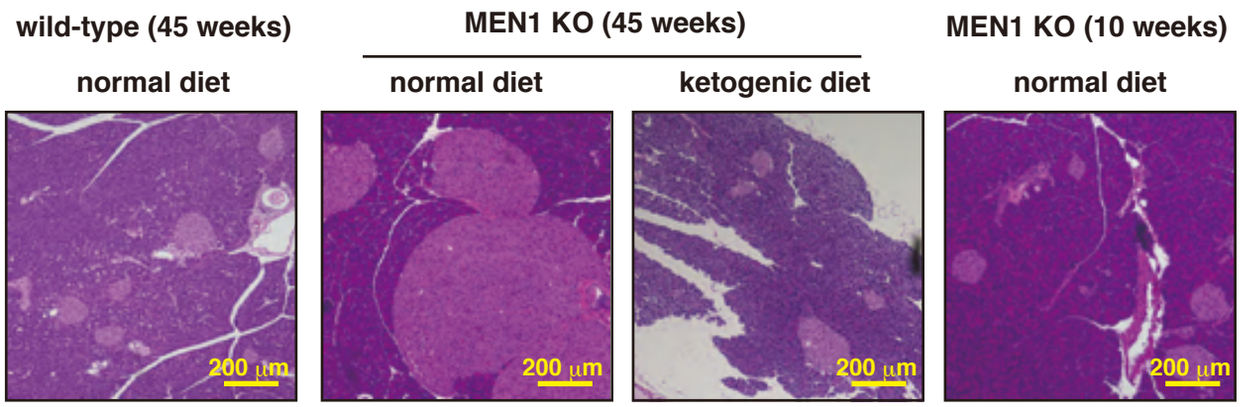

B

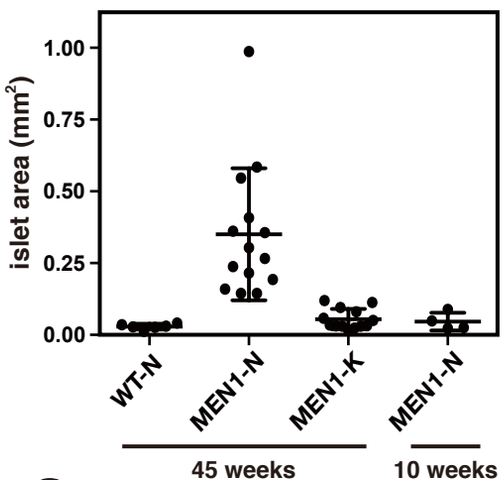

C

Tukey's multiple comparisons test	Summary	P Value
WT-N(45) vs. MEN1-N(45)	***	0.0004
WT-N(45) vs. MEN1-K(45)	ns	0.984
WT-N(45) vs. MEN1-N(10)	ns	0.998
MEN1-N(45) vs. MEN1-K(45)	****	< 0.0001
MEN1-N(45) vs. MEN1-N(10)	**	0.005
MEN1-K(45) vs. MEN1-N(10)	ns	1.000

D

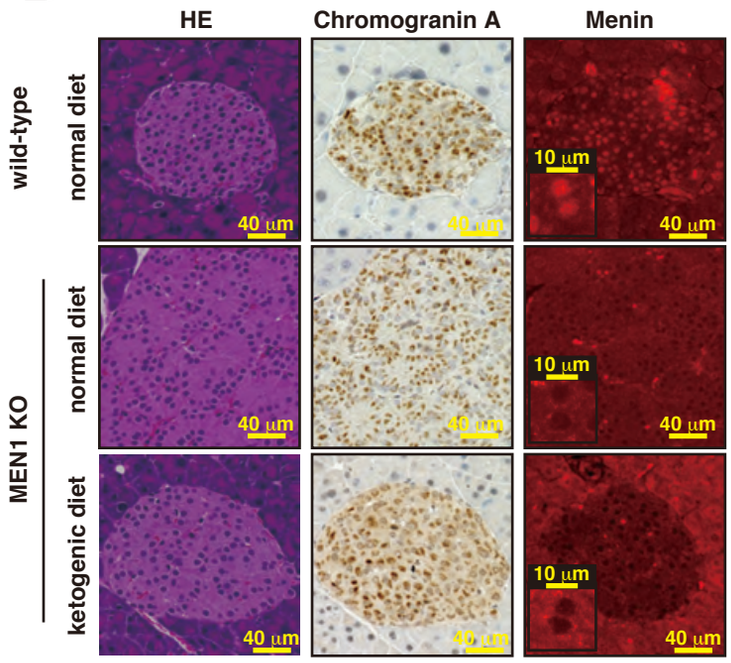

E

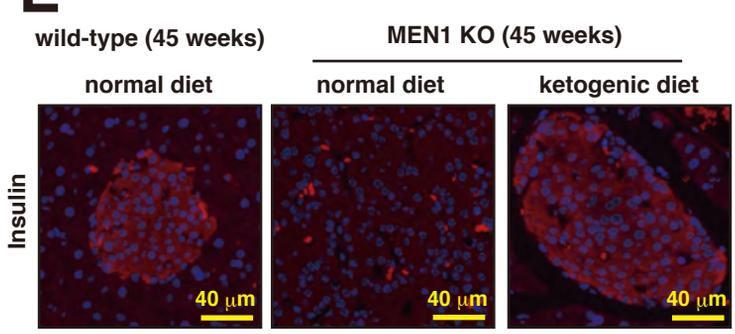

F

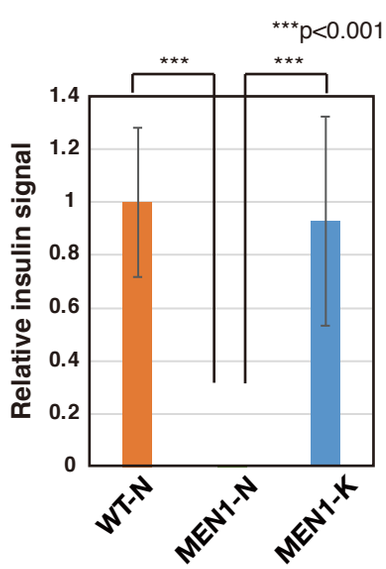

Fig. 3

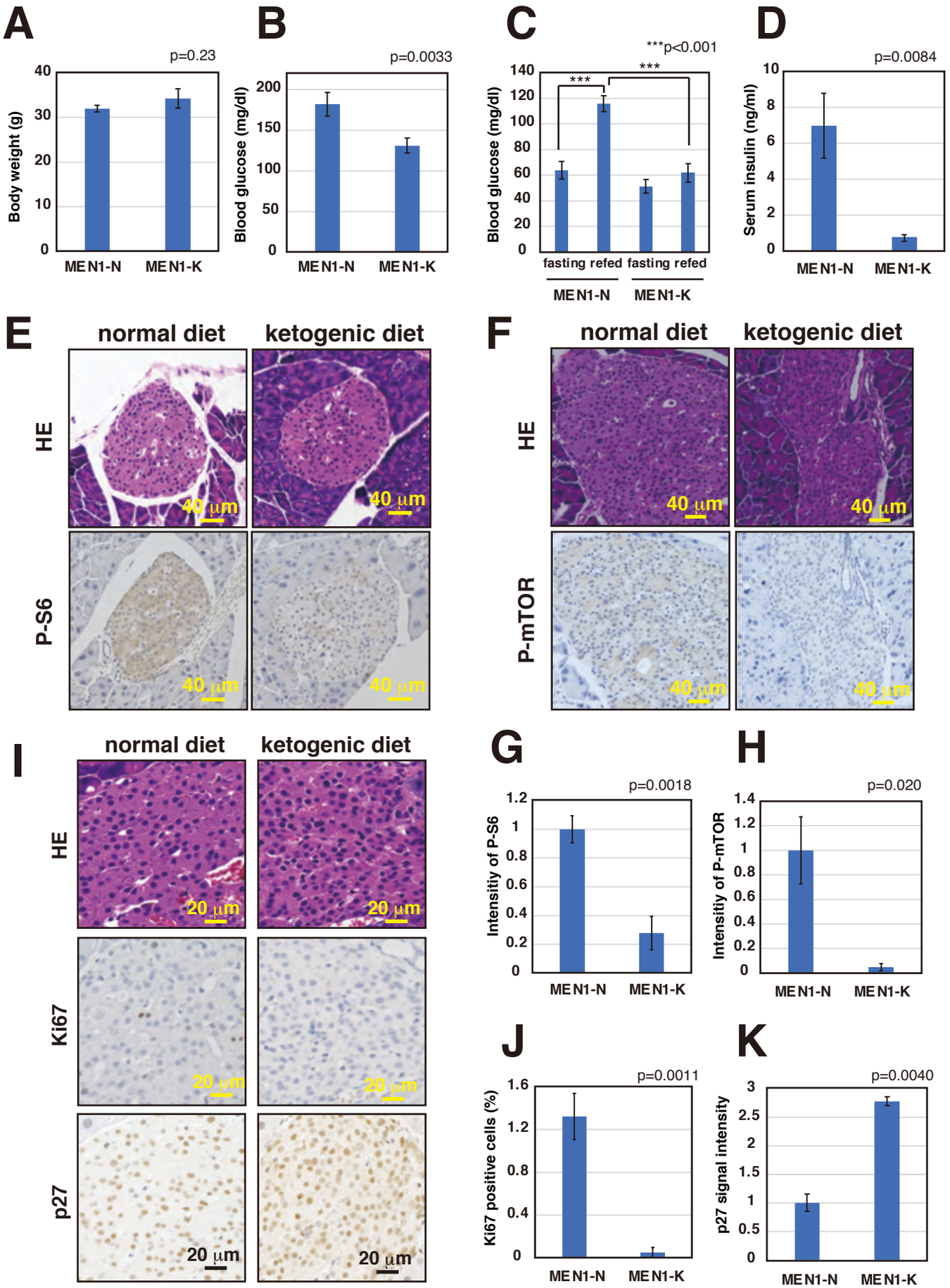
A
p=0.23
Body weight (g)
40
30
20
10
0
MEN1-N
MEN1-K
B
p=0.0033
Blood glucose (mg/dl)
200
150
100
50
0
MEN1-N
MEN1-K
C
***p<0.001
***
***
Blood glucose (mg/dl)
140
120
100
80
60
40
20
0
fasting refed fasting refed
MEN1-N
MEN1-K
D
p=0.0084
Serum insulin (ng/ml)
10
8
6
4
2
0
MEN1-N
MEN1-K
E
normal diet
ketogenic diet
HE
P-S6
40 μm
F
normal diet
ketogenic diet
HE
P-mTOR
40 μm
I
normal diet
ketogenic diet
HE
Ki67
p27
20 μm
G
p=0.0018
Intensitiy of P-S6
1.2
1
0.8
0.6
0.4
0.2
0
MEN1-N
MEN1-K
H
p=0.020
Intensitiy of P-mTOR
1.4
1.2
1
0.8
0.6
0.4
0.2
0
MEN1-N
MEN1-K
J
p=0.0011
Ki67 positive cells (%)
1.6
1.2
0.8
0.4
0
MEN1-N
MEN1-K
K
p=0.0040
p27 signal intensity
3
2.5
2
1.5
1
0.5
0
MEN1-N
MEN1-K

Fig. 4

A

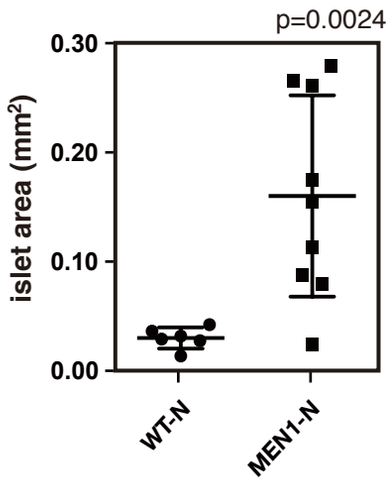

B

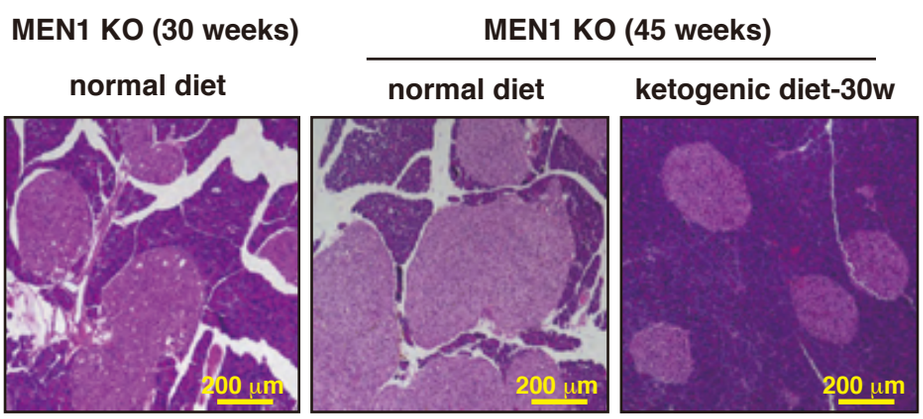

C

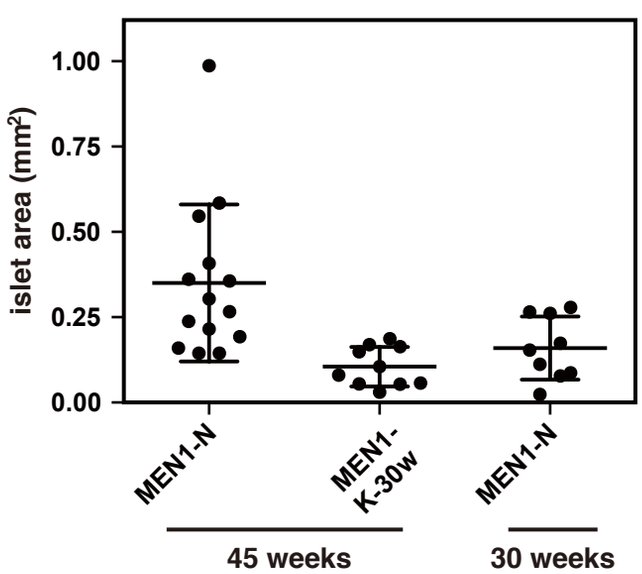

D

Tukey's multiple comparisons test	Summary	P Value
MEN1-N(45) vs. MEN1-K-30w(45)	**	0.003
MEN1-N(45) vs. MEN1-N(30)	*	0.026
MEN1-K-30w(45) vs. MEN1-N(30)	ns	0.748

Fig. 5

A

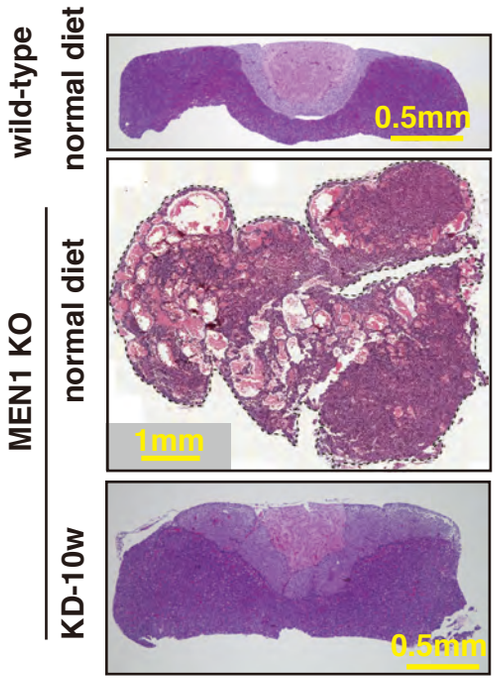

B

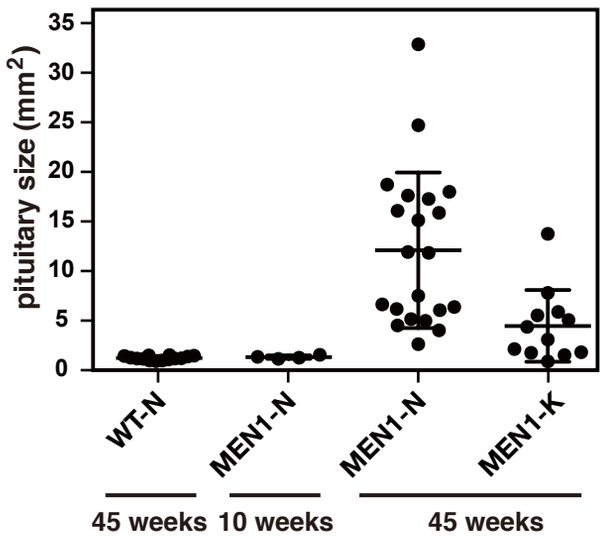

C

Tukey's multiple comparisons test	Summary	P Value
WT-N(45w) vs. MEN1-N(10w)	ns	> 0.9999
WT-N(45w) vs. MEN1-N(45w)	****	< 0.0001
WT-N(45w) vs. MEN1-K10w(45w)	ns	0.4324
MEN1-N(10w) vs. MEN1-N(45w)	***	0.0036
MEN1-N(10w) vs. MEN1-K10w(45w)	ns	0.7475
MEN1-N(45w) vs. MEN1-K10w(45w)	***	0.0017

D

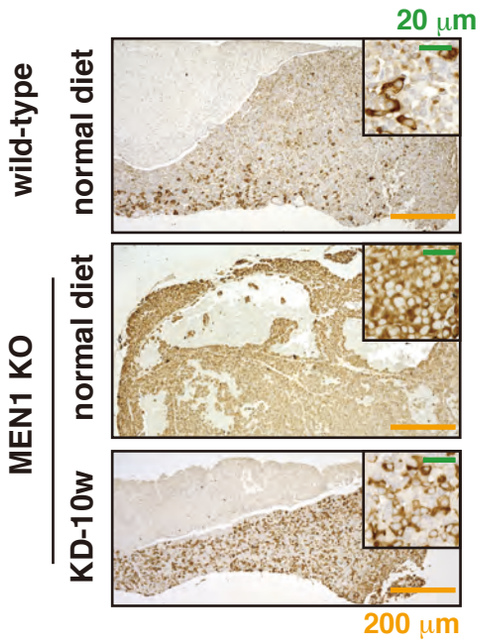

E

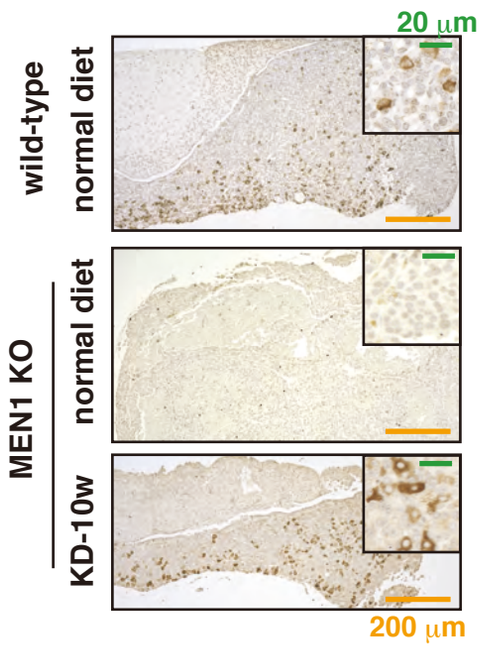

F

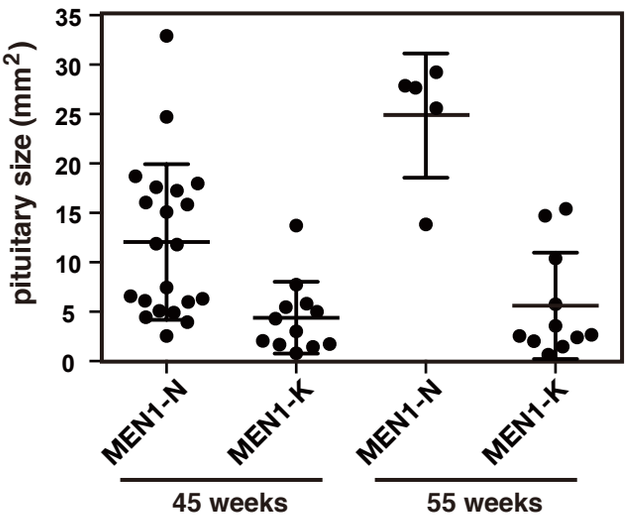

G

Tukey's multiple comparisons test	Summary	P Value
MEN1-N(45w) vs. MEN1-K-10(45w)	**	0.0094
MEN1-N(45w) vs. MEN1-N(55w)	**	0.0012
MEN1-N(45w) vs. MEN1-K-10w(55w)	*	0.0444
MEN1-K-10w(45w) vs. MEN1-N(55w)	****	< 0.0001
MEN1-K-10w(45w) vs. MEN1-K-10w(55w)	ns	0.9688
MEN1-N(56-59w) vs. MEN1-K-10w(55w)	****	< 0.0001

Fig. 6

A

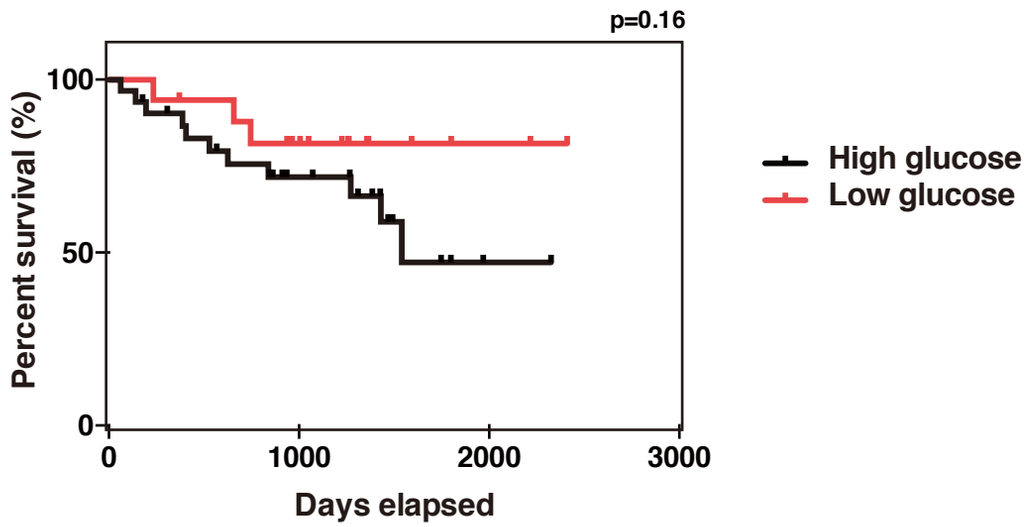

B

Parameters	Blood glucose		p value
	high (n=35)	low (n=21)	
Sex, n (%)			
Male	16 (70%)	7 (30%)	p=0.41
Female	19 (58%)	14 (42%)	
Age, n (%)			
<median (61 years)	19 (68%)	9 (32%)	p=0.58
≧median (61 years)	16 (57%)	12 (43%)	
Tumor grade, n (%)			
G1	3 (67%)	1 (33%)	
G2	26 (59%)	18 (41%)	p=0.70
G3	6 (75%)	2 (25%)	

C

Treatment, n (%)	Blood glucose	
	high (n=35)	low (n=21)
octreotide	4 (100%)	0 (0%)
lanreotide	11 (61%)	7 (39%)
everolimus	8 (80%)	2 (20%)
sunitinib	2 (67%)	1 (33%)
streptozotocin	4 (57%)	3 (43%)
lanreotide+everolimus	4 (67%)	2 (33%)
lanreotide+sunitinib	0 (0%)	4 (100%)
others	2 (67%)	1 (33%)